Journal of Nuclear Materials 383 (2008) 137–143

Contents lists available at ScienceDirect

Journal of Nuclear Materials

journal homepage: www.elsevier.com/locate/jnucmat

Extending the application range of a fuel performance code from normal operating to design basis accident conditions

P. Van Uffelen [a,*], C. Győri [a], A. Schubert [a], J. van de Laar [a], Z. Hózer [b], G. Spykman [c]

[a] European Commission, Joint Research Centre, Institute for Transuranium Elements, P.O.B. 2340, D-76125 Karlsruhe, Germany
[b] KFKI Atomic Energy Research Institute (AEKI), Hungary
[c] TÜV NORD EnSys Hannover GmbH & Co. KG, Germany

ARTICLE INFO

PACS:
28.41.Ak

ABSTRACT

Two types of fuel performance codes are generally being applied, corresponding to the normal operating conditions and the design basis accident conditions, respectively. In order to simplify the code management and the interface between the codes, and to take advantage of the hardware progress it is favourable to generate a code that can cope with both conditions. In the first part of the present paper, we discuss the needs for creating such a code. The second part of the paper describes an example of model developments carried out by various members of the TRANSURANUS user group for coping with a loss of coolant accident (LOCA). In the third part, the validation of the extended fuel performance code is presented for LOCA conditions, whereas the last section summarises the present status and indicates needs for further developments to enable the code to deal with reactivity initiated accident (RIA) events.

1. Introduction

In order to ensure the safe and economic operation of fuel rods, it is necessary to be able to predict their behaviour and to verify compliance with safety criteria under both normal operation and postulated accidents. The accurate description of the fuel rod's behaviour, however, involves various disciplines such as nuclear and solid state physics, metallurgy, ceramics, applied mechanics and the thermal heat transfer. The strong interrelationship of these disciplines calls for the development of computer codes describing the general fuel behaviour, such as the TRANSURANUS code [1]. Fuel designers and safety authorities rely heavily on this type of codes since they require minimal costs in comparison with the costs of an experiment or an unexpected fuel rod failure. Nevertheless, two types of fuel performance codes are generally being applied, corresponding to the normal operating and the design basis accident conditions (e.g. LOCA and RIA), respectively. In order to simplify the code management by limiting the number of programs and in order to take advantage of the hardware improvements, one should generate a single fuel performance code that can cope with the different conditions.

On the one hand, extending the application range of a fuel performance code originally developed for steady-state conditions to accident conditions requires modifications to the basic equations in the thermal-mechanical description of the fuel rod behaviour [2], stable numerical algorithms and a proper time step control, in addition to the implementation of specific models dealing with the high temperature behaviour of cladding such as observed under LOCA conditions [3]. For dealing with RIA events, one should check carefully the thermal expansion model because of the edge-peaked power distribution, as well as the other models affecting the effective cold gap width [4], as well as the model for thermal heat transfer in the plenum. On the other hand, for fuel performance codes developed to simulate some aspects of the nuclear fuel behaviour under accident conditions, such as TESPA [5], MFPR [6], or FRAPTRAN [7], either the thermo-mechanical behaviour of the fuel must be incorporated and/or the extension of models to normal operating conditions is necessary to consider burnup dependent phenomena such as thermal conductivity degradation, fission gas release and swelling as well as cladding corrosion. Such *a posteriori* modifications of the fuel performance code may entail difficulties in terms of convergence and calculation time.

Thanks to a clearly defined mechanical and mathematical framework as well as a consistent modelling, the TRANSURANUS fuel performance code has been able to cope with normal, off-normal and accidental operating conditions right from the beginning in 1973. It has a materials data bank for oxide, mixed oxide, carbide, and nitride fuels, Zircaloy and steel claddings, and different coolants. Options for a probabilistic analysis are also involved in order to provide for the possibility of a statistics-based evaluation. Despite the fact that the numerical solution techniques enable handling of non-steady-state conditions, and as such provide an ideal framework for a code to handle all conditions, some of the

* Corresponding author.
E-mail address: Paul.Van-Uffelen@ec.europa.eu (P. Van Uffelen).

0022-3115/$ - see front matter © 2008 Published by Elsevier B.V.
doi:10.1016/j.jnucmat.2008.08.043

phenomena important for design basis accidents (DBA) were not incorporated. As a first step towards this goal, a project was launched in order to extend the TRANSURANUS code capabilities to LOCA conditions [8]. This project focused on the simulation of the Zr1%Nb cladding performance under LOCA conditions and had two main objectives: (1) the compilation of a new database containing VVER-specific experiments to provide an appropriate background for model development and code validation [9] and (2) the improvement of the TRANSURANUS fuel performance code via the incorporation of newly developed correlations for off-normal conditions. Extensive code validation computations and the applications in the safety analyses of VVERs were also carried out in the project. In parallel to this project, similar models for Western type PWRs have been implemented and tested as well [10]. In a follow-up project, the hydrogen uptake of Zr1%Nb cladding and its effect on the oxidation and mechanical strength are being addressed. The need to launch this project stems from the observations of the cleaning tank incident at the Paks NPP [11], indicating that hydrogen uptake played a significant role in the mechanical deterioration of the cladding material. This effect, however, was not accounted for in the thermo-mechanical computations of the fuel performance code. In order to tackle this problem, both an experimental programme and a plan for model developments were launched.

In the second part of the paper, we present the model developments carried out for extending the application range of the TRANSURANUS code to LOCA conditions in a Russian type VVER as well as in a Western type PWR. Some of the experimental results on which these developments are based have been published previously [12]. In the third part of the paper, the validation of the extended code version is presented, whereas the fourth and last part outlines the needs for dealing with RIA events by means of the TRANSURANUS code.

2. Model developments

The prediction of the extent of cladding oxidation and hydrogen uptake, the crystallographic phase transition of zirconium, the plastic deformation of the overheated cladding as well as its rupture and ductility under LOCA conditions, is a key issue in safety analyses of pressurized water reactors. In order to assist the safety evaluation of VVER and PWR nuclear fuels, new deformation and oxidation rate correlations as well as adequate failure criteria were developed and incorporated into the TRANSURANUS fuel performance code for Zr1%Nb cladding at AEKI [8], while correlations from the open literature were incorporated for Zircaloy-4 by TÜV NORD [10].

2.1. Oxidation rate

The cladding-steam reaction model is based on parabolic kinetic correlations for both the oxygen mass gain and ZrO_2 layer thickness growth. The actual reaction rate constant is defined as a function of the temperature through an Arrhenius relation:

$$K_m = 658\exp(-10200/T), \tag{1}$$

where K_m is the oxygen mass gain rate in mg/cm^2/s$^{0.5}$ and T is the cladding temperature in K. The above equation is obtained by least–square fitting to experimental data for the oxygen mass gain rate of Zr1%Nb cladding in the temperature range of 500–1200 °C. In addition to this AEKI best-estimate relation, the Zr1%Nb-specific Solyany model [13,14] was incorporated. For standard Zircaloy-4 oxidation, the Baker–Just correlation [14,15], the Leistikow correlation [15] and the Cathcart–Pawel model [16] were also incorporated into the TRANSURANUS code, which can be chosen as an option.

From the recent set of oxidation experiments at AEKI with varying steam to hydrogen ratios, one could conclude that increasing the hydrogen content resulted in a reduced reaction rate constant for Zr1%Nb:

$$K_m = 117\exp(-8680/T). \tag{2}$$

Its dependency on the hydrogen partial pressure was smaller than the experimental uncertainties in the range of hydrogen contents under consideration (up to 36 vol.%).

2.2. Hydrogen uptake

A fraction of the hydrogen accompanying the Zr-steam reaction in LWRs under DBA conditions is absorbed by the cladding. Hydrogen absorption is known to enhance cladding embrittlement. It takes place during the oxidation process, or from a hydrogen-rich atmosphere under steam starvation conditions in a later phase of an accident. Experiments have indicated that the intensities of these two phenomena are different. In order to predict the hydrogen concentration in the cladding under both conditions, a simple hydrogen uptake model has been developed for Zr1%Nb that considers steam oxidation and steam starvation conditions (or H_2-rich environment) separately. In line with the high temperature oxidation model, the content of hydrogen uptake is computed incrementally with a quasi-stationary approach [9,13,14,17]:

$$C_{H,i} = \sqrt{C_{H,i-1}^2 + k^2\Delta t}, \tag{3}$$

where $k^2 = 2\eta C_s^2$, η is the kinetics constant, C_s represents the hydrogen solubility limit at a given temperature, Δt is the time step length, and the indices i and $i-1$ denote the actual and previous time steps, respectively. The main difference between the hydrogen uptake in steam or under H_2-rich atmosphere (steam starvation conditions) considered in the present model is the model constants:

$$\eta = \eta_0\exp\left(-\frac{Q_\eta}{T}\right) \tag{4}$$

and

$$C_s = \frac{K_s}{1+\frac{K_s}{M}}, \tag{5}$$

where the solubility constant K_s has to be multiplied by the square root of the hydrogen pressure in the event of a H_2-rich atmosphere and is expressed as follows:

$$K_s = \exp\left\{-\frac{\Delta H_0+\delta H}{RT}+\frac{\Delta S_0+\delta S}{R}\right\}, \tag{6}$$

$$\begin{aligned}\delta H &= R\cdot B\cdot C_o,\\ \delta S &= R\cdot\ln(1-A\cdot C_o),\end{aligned} \tag{7}$$

where C_o represents the ratio of oxygen to zirconium atoms, M indicates the total number of interstitial sites for hydrogen dissolution per Zr atoms, and the molar quantities of enthalpy and entropy were fitted to experimental data for Zr1%Nb (see Table 1).

2.3. Phase transition model

The $\alpha \rightarrow \beta$ phase transition of zirconium takes place principally in the temperature range of 800–1000 °C, which is typical in a LOCA. The phase transformation is not only temperature dependent, but is also influenced by the composition and the impurities of the alloy, the corrosion level (oxygen and hydrogen contents) of the cladding and the temperature increase rate. In the TRANSURANUS code the fractions of the metallurgical phases are calculated by two optional models representing static or dynamic approaches through empirical functions.

Table 1
Fitted parameters for the hydrogen uptake model of Zr1%Nb in the TRANSURANUS code

Parameter	H_2-rich atmosphere	Steam oxidation
η (s^{-1})	0.1033	20537
Q_η (K)	5140	23600
ΔH_0 (J/mol)	−63860	−77653
ΔS_0 (J/mol/K)	−97.39	−76.07
M	2.5	2.5
A	2.0	2.0
B	3088	3088

Quasi equilibrium conditions are assumed in the static model where the fraction of the β phase (φ) is a simple function of the temperature, $\varphi = f(T)$. Specific functions were established for each alloy. Fig. 1 represents these functions for Zircaloy-4 and for Zr1%Nb, indicating that due to the niobium content the phase transition of zirconium is completed at temperatures about 100 °C lower.

The optional dynamic model, implemented by the TÜV Hannover, is based on Forgeron's approach [18] to simulate the effect of the temperature variation rates on the phase transitions. The kinetics of the $\alpha \rightarrow \beta$ transformation is described by the following differential equation:

$$\frac{d\varphi}{dt} = K(T) \cdot \varphi \cdot (1 - \varphi), \tag{8}$$

where $K(T)$ is an appropriate function of the temperature in the form:

$$K = \pm |T - f^{-1}(\varphi)| \cdot \exp(C_1 + C_2 \cdot |T - f^{-1}(\varphi)|), \tag{9}$$

t is the time, C_1 and C_2 are empirical constants. The fraction of the β phase is calculated by applying the Euler-explicit integration:

$$\varphi_i = \varphi_{i-1} + K(T_i, \varphi_{i-1}) \cdot \varphi_{i-1} \cdot (1 - \varphi_{i-1}) \cdot \Delta t, \tag{10}$$

where the indices i and $i-1$ denote the actual and the previous time steps, respectively and the time step increase is limited in the code in order to avoid numerical instability. As an example, Fig. 1 also represents a hysteresis loop of the phase transition calculated for Zircaloy-4 by means of the dynamic model at ±10 °C/s heating/cooling rates.

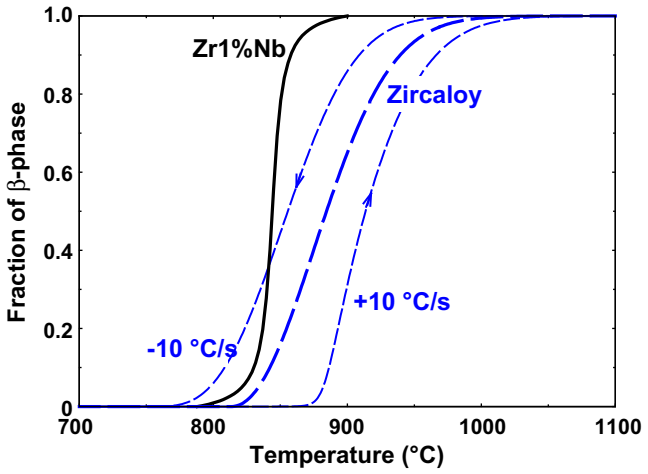

Fig. 1. Fraction of the β phase as a function of temperature calculated by the equilibrium model for Zircaloy-4 and Zr1%Nb and by the dynamic model for Zircaloy-4 at ±10 °C/s temperature rates.

2.4. Clad deformation rate model

The one-dimensional mechanical model of the TRANSURANUS code is based on a semi-analytic solution of the principal mechanical equations for the radial deformation (i.e. the expressions of the non-elastic strains involved in the analytic formula are integrated numerically along the radius). The non-elastic strain components are calculated incrementally in time. The increments of the equivalent creep or plastic strain can be defined through an optional non-linear function of the equivalent stress. In conformity with this model, the large plastic deformation (i.e. ballooning) of the cladding was defined by strain rate correlations in the form of a Norton power equation [8,19],

$$\dot{\bar{\varepsilon}} = \frac{d\bar{\varepsilon}}{dt} = A \cdot \exp\left(\frac{-Q}{R \cdot T} + B(x)\right) \cdot \bar{\sigma}^n, \tag{11}$$

where $\dot{\bar{\varepsilon}}$ is the effective strain rate, $\bar{\sigma}$ is the effective stress, R is the universal gas constant, T is the temperature, A is the strength coefficient, Q is the activation energy for the plastic deformation, n is the stress exponent, and $B(x)$ is a third degree polynomial of the oxygen weight concentration of the cladding (x).

2.4.1. Norton parameters and effect of oxygen

The parameters of the Norton equation (A, Q and n), as well as the function accounting for the effect of the cladding oxidation, were defined separately for the α and the β phases of the different cladding alloys. The appropriate Norton parameters for Zircaloy-4 were defined by Erbacher on the basis of REBEKA test data [20]. The Norton parameters and $B(x)$ for the Zr1%Nb cladding were fitted to the data of independent cladding burst tests performed at the AEKI [12] and at the Kurchatov Institute (Russia) [21]. The parameter optimization was carried out for two temperature intervals, 600–800 °C and 900–1200 °C, corresponding to the different crystallographic phases of the Zr1%Nb alloy (see Tables 2 and 3).

2.4.2. Strain rate in the α–β phase transition range

In order to define the effective strain rate of the cladding in the metallurgical phase transition range there are two different approaches applied in the TRANSURANUS code. According to the first approach, implemented by the TÜV Hannover for Zircaloy-4 [10,22], the Norton parameters are interpolated in the transition range using the fractions of the α and β phases as weighting factors:

Table 2
Norton parameters for Zircaloy-4 and Zr1%Nb claddings

		A ($MPa^{-n}\,s^{-1}$)	n (−)	Q (J/mol)
Zircaloy-4	α-Phase	8.7×10^3	5.89	$3.21 \times 10^5 + 24.69 \cdot (T - 923.15)$
	β-Phase	7.9	3.78	1.42×10^5
Zr1%Nb	α-Phase	6.1×10^6	5.18	3.6×10^5
	β-Phase	1.4	5.82	1.8×10^5

Table 3
Polynomial coefficients for the oxygen concentration term of the Zr1%Nb-specific strain rate correlation

		c_3	c_2	c_1	c_0
α-Phase	$0 < x < 0.02$	-6.7×10^5	4.9×10^4	-5.7×10^2	0
	$0.02 \leqslant x < 0.1$	2.3×10^4	-6.4×10^3	7.4×10^2	−9.5
β-Phase	$0 < x < 0.02$	-7.4×10^5	5.5×10^4	-6.3×10^2	0
	$0.02 \leqslant x < 0.1$	2.6×10^4	-7.1×10^3	8.2×10^2	−10.5

$$\ln(A_{\alpha\beta}) = (1-\varphi)\cdot\ln(A_\alpha) + \varphi\cdot\ln(A_\beta),$$
$$Q_{\alpha\beta} = (1-\varphi)\cdot Q_\alpha + \varphi\cdot Q_\beta, \quad (12)$$
$$n_{\alpha\beta} = (1-\varphi)\cdot n_\alpha + \varphi\cdot n_\beta.$$

The second approach, applied for Zr1%Nb, is based on micro-mechanical considerations for composite materials assuming a statistically homogeneous distribution of α-phase inclusions embedded in the β phase matrix, i.e. each representative volume element has the same α–β volume fraction corresponding to the macroscopic average value. According to the basic relation of self-consistency [23] the overall average strain, and consequently the macroscopic strain rate of the two-phase cladding ($\dot{\varepsilon}_{\alpha\beta}$) is expressed as the weighted average of the strain rates of each phases:

$$\dot{\varepsilon}_{\alpha\beta} = (1-\varphi)\cdot\dot{\varepsilon}_\alpha + \varphi\cdot\dot{\varepsilon}_\beta. \quad (13)$$

2.5. Cladding failure criteria

For the simulation of fuel rod performance under postulated accidents, the implementation of an appropriate cladding failure criterion is essential. The cladding failure is generally predicted on the basis of a stress assessment, i.e. the comparison of the calculated tangential stress with a distinct failure threshold. However, due to the significant uncertainty of the stress computation at large cladding deformation, a strain-based failure criterion can be more appropriate for LOCA conditions. By considering both of these possibilities, two optional criteria were incorporated into the TRANSURANUS code.

The first (standard) criterion is a typical stress-based evaluation: cladding failure is indicated when the true tangential stress (σ_{tB}) exceeded the threshold stress defined on the basis of experimental data, as illustrated in Fig. 2. The effect of cladding oxidation on the true burst stress is considered through the multiplication factor which is an exponential function of the average oxygen concentration in the cladding (including the oxide layer).

The Zr1%Nb-specific function was fitted to experimental data. The failure threshold applied for Zircaloy-4 is derived from the literature [24].

The second failure principle is a simple plastic instability criterion based on the simultaneous assessment of the effective true strain and the strain rate. When both the strain and the strain rate exceed the threshold values of 0.02 and 100 1/h, respectively, the cladding is assumed to be ruptured.

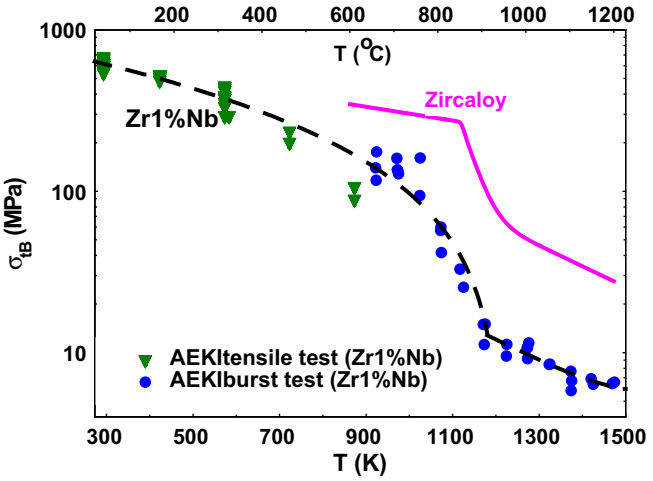

Fig. 2. True tangential stress at burst as a function of temperature applied as failure limit for un-oxidised Zr1%Nb and Zircaloy-4 claddings.

2.6. Cladding ductility

In order to assess the capability of the cladding to withstand the thermal stress during the quenching phase of a LOCA event, it is important to know when the ductile–brittle transition occurs. In order to preserve fuel rod integrity, the current safety criteria require the maximum local equivalent cladding reacted (ECR) and the peak cladding temperature to remain below 17% and 1200 °C, respectively. However, these criteria are being re-analysed in view of new experimental evidence and because new materials are being proposed to meet the requirements of higher discharge burnup values. AEKI has proposed a new approach [9,25], based on defining a cladding ductility parameter that is computed incrementally and compared against a limit corresponding to the ductile–brittle transition. Cladding ductility is guaranteed if

$$P_i = \sqrt{P_{i-1}^2 + \lambda^2\Delta t} < 1 \quad (14)$$

and becomes brittle when P exceeds 1, where P_i and P_{i-1} are the so-called ductility parameters in the actual and previous time step respectively, Δt is the time step length (s) during which the temperature is assumed to remain constant, λ^2 represents the square of the rate constant or ductility limit derived from ring compression tests with oxidised Zircaloy-4 and Zr1%Nb specimens:

$$\lambda_{Zy4}^2 = 10^4\exp(-\frac{20\,000}{T}),$$
$$\lambda_{Zr1\%Nb}^2 = 5\times10^3\exp(-\frac{17\,500}{T}). \quad (15)$$

Note that the reciprocal of the rate constant λ^2 corresponds to the time of oxidation (*t, expressed in s*) after which the cladding becomes brittle for a given temperature.

The nature of the failure is determined by integrating the load–displacement curves of the standard ring compression tests until the first indication of failure, and comparing the integral to an energy limit. When the specific energy at failure, i.e. the energy at failure per unit height of the ring, exceeds 50 mJ/mm the cladding was observed to fail in a brittle way, which is indicated in Fig. 3 with an empty symbol. Sorting the specimens on the basis of the calculated specific energy, it was possible to determine the line corresponding to the ductile–brittle transition separately for Zry-4 and Zr1%Nb.

Although the hydrogen uptake strongly reduced the ductility of the cladding in terms of specific energy at failure (Fig. 4), the ductility limit or ductile–brittle transition time during oxidation was shown to be independent of the hydrogen content in the atmosphere. The slowing down of the oxidation therefore seems to compensate for the mechanical deterioration of the cladding when the hydrogen uptake increases.

3. Validation of the extended TRANSURANUS code

The validation of the extended TRANSURANUS code for LOCA analyses has, in a first step, included the comparison of the code results with analytic solutions of simplified cases (e.g. isothermal conditions), and in a second step the simulation of separate effect cladding oxidation and ballooning tests. In a third step, the TRANSURANUS code is applied in a benchmark exercise organised by the OECD NEA to predict the behaviour of PWR and VVER fuel rods in an integral LOCA tests performed at the OECD Halden Reactor Project.

3.1. Simulation of cladding oxidation tests

A total of 122 cladding oxidation tests performed in a steam atmosphere in the temperature range of 500–1200 °C were simu-

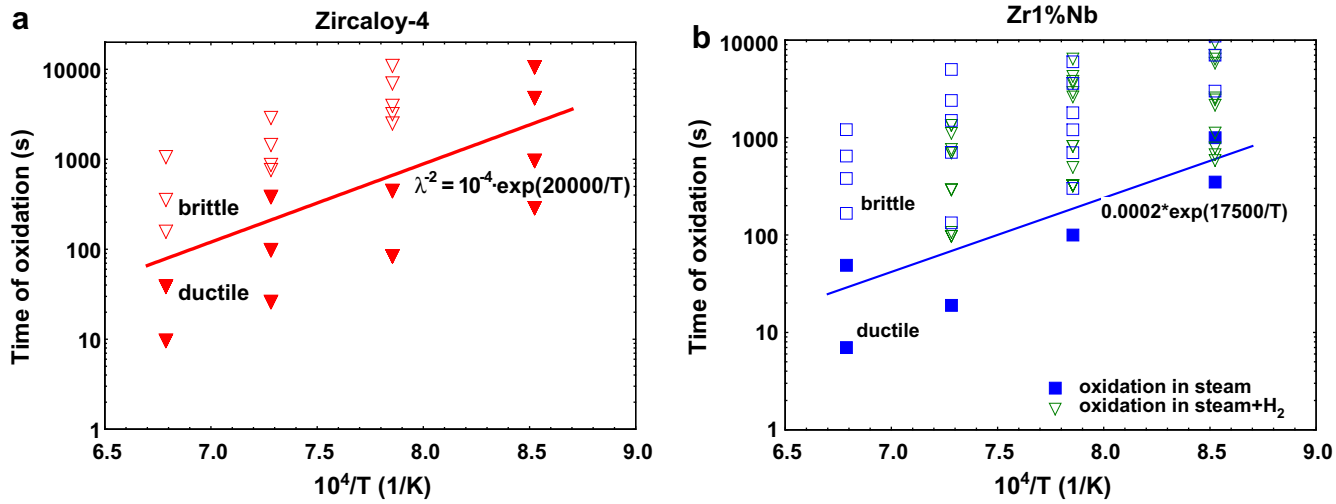

Fig. 3. Time of oxidation versus the reciprocal of the oxidation temperature, indicating the limit between the ductile and brittle behaviour in standard Zircaloy-4 (a) and Zr1%Nb (b) claddings.

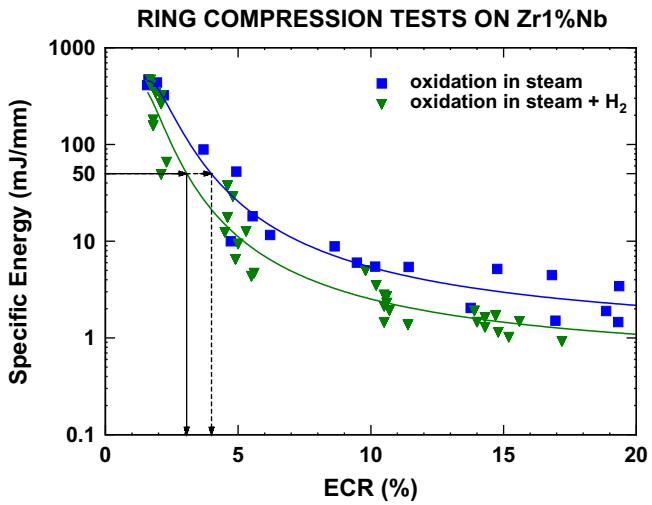

Fig. 4. Specific energy at failure, derived from standard ring compression tests, versus the measured oxidation ratio for Zr1%Nb cladding.

lated by the TRANSURANUS code. The oxidation of the Zr1%Nb specimens was calculated using both the AEKI best-estimate and the Solyany reaction rate correlations. The evaluation of the simulations was based on the comparison of the calculated and the measured oxygen mass gain data. The results are presented in Fig. 5. The satisfactory agreement between the calculations and the measurements is evident; however, two tendencies can be observed: (1) The Solyany reaction rate correlation results in a general slightly over-predicted mass gain as compared to the experimental data. This indicates the conservatism of the Solyany model in the computation of the equivalent cladding oxidation. (2) The computation with the AEKI correlation slightly over-predicts the mass gain at moderate oxidation, when the cladding temperature is below 900 °C or the exposition time is very short, but is accurate for greater oxidation conditions.

3.2. Simulation of cladding burst tests

The core of the code validation was based on the post-test analyses of nearly 400 cladding burst tests representing a wide scope of

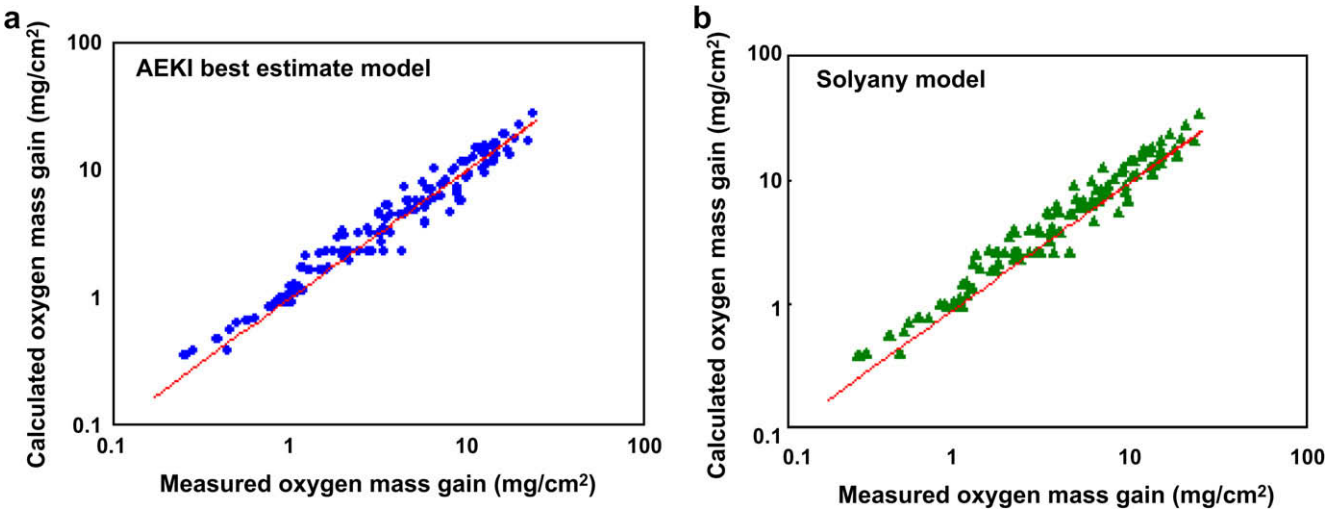

Fig. 5. Calculated versus measured oxygen mass gain. The computations were carried out with the AEKI oxidation rate correlation (Fig. 5(a)) and with the Solyany oxidation rate correlation (Fig. 5(b)).

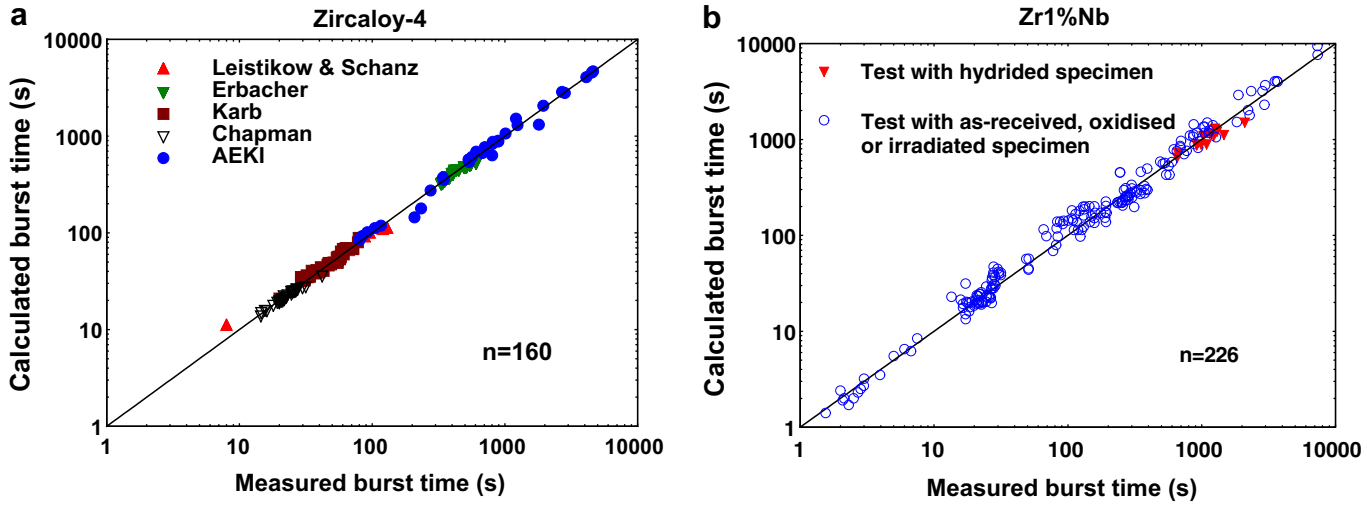

Fig. 6. Calculated versus measured times to cladding burst for standard Zry-4 tubes (Fig. 6(a)) and for 226 Zr1%Nb tubes (Fig. 6(b)). The tests for Zr1%Nb contain the recent hydrogen-charged specimen tested by AEKI.

LOCA conditions with varying pressurization rate, temperature increase rate and oxidation level. Tests of different institutes, e.g. AEKI [12], the Kurchatov Institute (KI) or the Forschungszentrum Karlsruhe (FZK), performed with Zircaloy-4 and Zr1%Nb cladding specimens in the temperature range of 600–1200 °C were selected for the validation [9]. The tests were carried out with as-fabricated, pre-oxidised or irradiated segments in inert gas or steam atmosphere. The two most recent series of burst tests at AEKI involved 100 mm long pre-oxidised tube specimens that had been hydrided prior to the pressurisation. Since the measured tangential strains have a wide spread, the evaluation is based on the comparison of the calculated and the measured times of cladding burst. Fig. 6 represents the calculated versus the measured time of burst for the Zr1%Nb and for the Zircaloy-4 segments, separately. The results are convincing as they indicate reliable TRANSURANUS simulation for a wide range of situations representing slow as well as fast experiments.

3.3. Simulation of an integral test

The TÜV Hannover has also applied the TRANSURANUS code for the simulation of the Halden integral LOCA tests performed with fresh and high burnup PWR fuel rods. The result shown in Fig. 7 corresponds to an experiment that was carried out with a fresh, pressurized PWR rod in a high pressure loop of the reactor. The maximum cladding temperature and the temperature increase rate were 1050 °C and 5–7 °C/s, respectively. Fuel rod ballooning started at about 80 s after the initiation of the blow-down when the cladding temperature reached 800 °C. The measured coolant pressure history and the cladding temperature history, derived from detailed thermohydraulic analysis, were used as boundary conditions for the TRANSURANUS simulation. The results reveal that the rod internal pressure, the cladding circumferential deformation as well as the subsequent burst were calculated correctly, as illustrated in Fig. 7.

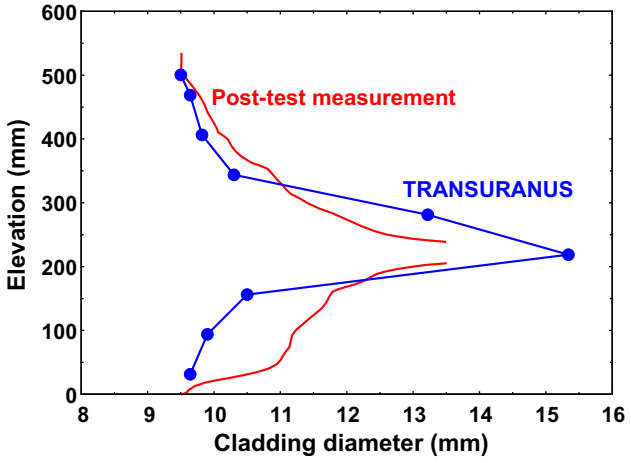

Fig. 7. Cladding deformation profiles measured after a Halden LOCA test and calculated by the TRANSURANUS code.

4. Summary and conclusions

In order to simplify the code management and the interface between the codes, and to take advantage of the hardware progress it is necessary to generate a code that can cope with both normal operating and design basis accident conditions. Thanks to a clearly defined mechanical–mathematical framework and a consistent modelling, the TRANSURANUS fuel performance code was designed to be able to cope with normal, off-normal and accidental operating conditions right from the beginning in 1973. Nevertheless, the extension of the application range of the code to design basis accident conditions such as LOCA and RIA required specific models to be developed and implemented. In a first step, models for dealing with a LOCA have been implemented and tested. They include new Zry-4- and Zr1%Nb-specific models for the high temperature oxidation, the $\alpha \rightarrow \beta$ phase transformation, the plastic deformation and the failure of the fuel cladding under LOCA conditions. New correlations were developed for the Zr1%Nb cladding alloy considering the interference between cladding oxidation, strain rate and mechanical strength. A new method for the evaluation of cladding embrittlement has also been introduced as an alternative to the zero ductility criterion related to 17% cladding oxidation.

The new and extended version of the TRANSURANUS code is being transmitted to the user community, after having been validated on the basis of post-test analyses of numerous cladding burst experiments that have proven the reliability of the TRANSURANUS code predictions for both PWR and VVER fuel rod performance in the temperature range of 600–1200 °C. The simulations of the Halden LOCA experiments in an OECD benchmark programme also confirm the applicability of the code in DBA analyses. However,

some further harmonisation of the Zry-4- and the Zr1%Nb-specific models concerning the strain rate and the failure stress in the $\alpha \rightarrow \beta$ phase transition range is envisaged for the consistent simulation of the different claddings by the same code. Furthermore, experiments for measuring the temperature shift of the phase change when varying the temperature rate are underway in order to model the phase change in Nb-containing cladding materials for Western and Russian type reactors with a dynamic model in a consistent manner. These refinements will be further tested against the experimental results of an integral LOCA test with a VVER fuel rod in the OECD Halden Reactor, as well as the experimental data made available through the FUMEX-II exercise of the IAEA and the IFPE database of the NEA.

In a second phase, the model capabilities will also be extended to RIA conditions, covering adapted models for

- the thermal expansion and the edge-peaked power distribution;
- the effective cold gap width (and all models affecting this width);
- the thermal heat transfer in the plenum.

A properly defined benchmark, for instance in the frame of a FUMEX-III from the IAEA, would be very welcome in this respect.

References

[1] K. Lassmann, J. Nucl. Mater. 188 (1992) 295.
[2] K. Lassmann, P. Van Uffelen, The Structure of Fuel Rod Codes, Publications Office, JRC Publications European Commission, 2004, EUR 21400 EN.
[3] P. Van Uffelen, C. Bruynooghe, Cs. Győri, J. Jonnet, A. Schubert, J. van de Laar, in: Sixth International Conference on WWER Fuel Performance, Modelling and Experimental Support, Albena, Bulgaria, 19–23 September 2005.
[4] R.O. Meyer, in: International Meeting on LWR Fuel Performance, "Nuclear Fuel: Addressing the Future", Topfuel, Salamanca, Spain, 22–27 October 2006, p. 284.
[5] H.G. Sonnenburg, in: International Meeting on LWR Fuel Performance, "Nuclear Fuel: Addressing the Future", Topfuel, Salamanca, Spain, 22–27 October 2006, p. 467.
[6] M.S. Veshchunov, V.D. Ozrin, V.E. Shestak, V.I. Tarasov, R. Dubourg, G. Nicaise, Nucl. Eng. Des. 236 (2) (2006) 179.
[7] G.A. Berna, H. Scott, FRAPTRAN: A Computer Code for the Transient Analysis of Oxide Fuel Rods, US Nuclear Regulatory Commission, August 2001, NUREG/CR-6739.
[8] Cs. Győri, Z. Hózer, K. Lassmann, A. Schubert, J. van de Laar, M. Cvan, B. Hatala, in: EU Research in Reactor Safety, Conclusion Symposium on Shared-Cost and Concerted Actions (FISA-2003), Proceedings – EUR 21026, Luxembourg, 10–13 November 2003, p. 584.
[9] Cs. Győri, P. Van Uffelen, A. Schubert, J. van de Laar, Z. Hózer, in: Sixth International Conference on WWER Fuel Performance, Modelling and Experimental Support, Albena, Bulgaria, 19–23 September 2005.
[10] G. Spykman, D. Märtens, D. Bour, P. Kock, K. Lassmann, A. Schubert, J. van de Laar, in: Enlarged Halden Programme Group Meeting on High Burn-up Fuel Performance, Safety and Reliability, Sandefjord, Norway, 9–14 May 2004.
[11] G. Nagy, A. Somogyi, G. Patek, T. Pintér, R. Schiller, Ann. Nucl. Energy 34 (6) (2007) 496.
[12] Z. Hózer, Cs. Győri, M. Horváth, I. Nagy, L. Maróti, L. Matus, P. Windberg, J. Frecska, Nucl. Technol. 152 (3) (2005) 273.
[13] V.I. Solyany, Y.K. Bibilashvili, V.Y. Tonkov, in: OECD-NEA-CSNI/IAEA Specialists Meeting on Water Reactor Fuel Safety and Fission Product Release in Off-Normal and Accident Conditions, Risø, Denmark, 16–20 May 1983, p. 163.
[14] L. Baker, L.C. Just, in: Experimental and Theoretical Studies of Zirconium–Water Reaction, Argonne National Laboratory, Chicago, May 1962, ANL-6548.
[15] S. Leistikow, Hochtemperatur-Oxidation von Zircaloy-Hüllrohren in Wasserdampf, Abschlusskolloquium Project Nukleare Sicherheit Kernforschungszentrum Karlsruhe, 1986.
[16] G. Schanz, Recommendations and Supporting Information on the Choice of Zirconium Oxidation Models in Severe Accident Codes, Forschungszentrum Karlsruhe, Karlsruhe, 2003, FZKA 6827, SAM-COLOSS-P043.
[17] S. Leistikow, G. Schanz, Nucl. Eng. Des. 103 (1987) 65.
[18] T. Forgeron, J.C. Brachet, F. Barcelo, A. Castaing, J. Hivroz, J.P. Mardon, C. Bernaudat, in: 12th International Symposium: Zirconium in the Nuclear Industry, vol. ASTM STP 1354, West Conshohocken, 2000.
[19] V.J. Betten, Creep Mechanics, Springer, 2002. p. 327.
[20] M.E. Markiewicz, F.J. Erbacher, Experiments on Ballooning in Pressurised and Transiently Heated Zircaloy-4 Tubes, Kernforschungszentrum Karlsruhe, 1988, KfK-Bericht 4343.
[21] L. Yerogova, Data Base on the Behavour of High Burnup Fuel Rods with Zr1%Nb Cladding and UO_2 Fuel (WWER type) Under Reactivity Accident Conditions, Moscow, 1998, NUREG/IA-0156, NSI RRC 2179.
[22] G. Spykman, D. Maertens, D. Bour, in: International Workshop "Towards Nuclear Fuel Modelling in the Various Reactor Types Across Europe", Karlsruhe, 25–26 June 2007.
[23] R. Hill, J. Mech. Phys. Solids 13 (1965) 213.
[24] F.J. Erbacher, in: 12th International Symposium on "Zirconium in the Nuclear Industry", 1982.
[25] Z. Hózer, C. Győri, in: Special Expert Group Fuel Safety Margins (SEGFSM) Topical Meeting in LOCA Issues, Argonne, Illinois, USA, 2004.